JOURNAL OF AGRICULTURAL AND FOOD CHEMISTRY

J. Agric. Food Chem. **2006,** *54,* 5113−5119 **5113**

Characterization Using Raman Microspectroscopy of Arabinoxylans in the Walls of Different Cell Types during the Development of Wheat Endosperm

SULLY PHILIPPE,† CÉCILE BARRON,§ PAUL ROBERT,† MARIE-FRANÇOISE DEVAUX,† LUC SAULNIER,† AND FABIENNE GUILLON*,†

INRA—Unité de Recherches Biopolymères, Interactions et Assemblages, B.P. 71627, 44316 Nantes, France, and Unité mixte de Recherches Ingénierie des Agropolymères et Technologies Emergentes, INRA-ENSAM-UMII-CIRAD, 2 place Viala, 34060 Montpellier, France

The time course and pattern of arabinoxylan deposition in the wheat (*Triticum aestivum*) endosperm during grain development were studied using Raman spectroscopy. The presence of arabinoxylans (AX) is detected at the beginning of grain filling. At this stage, AX appear more substituted than at the later stages. Feruloylation of AX increases during the grain-filling stage, especially in the case of the aleurone layer. Whatever the stage of grain development, four populations of cells could be defined according to Raman arabinoxylan signatures. In the walls of the aleurone cells, AX appeared to be little substituted and highly esterified with phenolic acids. In the walls of prismatic cells, AX were found to be highly substituted and poorly esterified. Apart from aleurone and prismatic cells, the substitution degree of AX in endosperm was in the same range. Cells in the crease region were distinguished from cells in the starchy endosperm by their lower amount of esterified phenolic compounds.

KEYWORDS: Arabinoxylans; ferulic acid; endosperm development; Raman; PCA; *Triticum aestivum*

INTRODUCTION

Arabinoxylans (AX) are the main nonstarch polysaccharides of cell walls of mature wheat grain endosperm. They constitute 70% of the walls, which account in endosperm for 2−4% of dry weight. Many studies have focused on AX in relation with cereal technology and feedstuffs (*1*, *2*).

Wheat endosperm AX consist of a linear backbone of β (1→4) linked D-xylopyranosyl residues, which are unsubstituted (uXyl), monosubstituted (mXyl) at O-3, or disubstituted (dXyl) at O-3 and O-2 with α-L-arabinofuranosyl residues. Arabinosyl residues can be esterified with phenolic compounds, mainly ferulic acid. In wheat, ≈25% of AX are water extractable (WE-AX). WE-AX structure could be depicted by their arabinose-to-xylose ratio (A/X) (from 0.31 to 1.06) and by their degree of esterification with ferulic acid (0.2−0.4% of WE-AX, w/w) (*3*−*6*). The chemical structure of water unextractable AX (WU-AX, two-thirds of AX in endosperm cell walls) is very close to that of WE-AX (*7*). Nevertheless, WU-AX exhibit higher average molecular weight, slightly higher A/X ratio, and diferulate cross-links.

Local structural heterogeneity of AX within endosperm has been described. AX in the aleurone cell wall of mature endosperm are characterized by low A/X ratio in the range of 0.3−0.4 (*8*−*10*). Aleurone cell walls of mature endosperm are heavily esterified by ferulic acid (1.8%, w/w) compared to starchy endosperm cell walls (0.04%, w/w) (*6*, *8*−*10*). Using Fourier transform infrared microspectroscopy (micro-FTIR), Barron et al. (*11*) found differences in cell wall composition between the peripheral and central regions of the starchy endosperm. They suggested that differences were mainly due to AX.

Philippe et al. (*12*) reported that AX were synthesized at the beginning of the cell differentiation stage in wheat grain developing endosperm, but were missing in early development stages. Changes in the substitution degree of AX were observed within the future starchy endosperm as soon as the differentiation stage of wheat grain development took place (*12*).

Raman spectroscopy is well-known to provide complementary information compared to FT-IR on molecular vibrations (*13*−*16*). Whereas FT-IR spectroscopy mainly works with asymmetrical vibrations of covalent bonds, Raman spectroscopy is more sensitive to the symmetrical vibrations.

Both FT-IR microspectroscopy and Raman microspectroscopy have been shown to be powerful in the investigatation of in situ cell wall composition (*11*, *17*−*22*). With conventional equipment, one significant advantage of Raman to FT-IR microspectroscopy is the higher spatial resolution (*23*). Piot et al. (*22*) explored wheat endosperm cell walls in relation with grain cohesion using Raman microspectroscopy. The authors

* Author to whom correspondence should be addressed (e-mail guillon@nantes.inra.fr; telephone +33-2-40675016; fax +33-2-40675229).
† INRA.
§ IINRA-ENSAM-UMII-CIRAD.

10.1021/jf060466m CCC: $33.50
Published on Web 06/15/2006

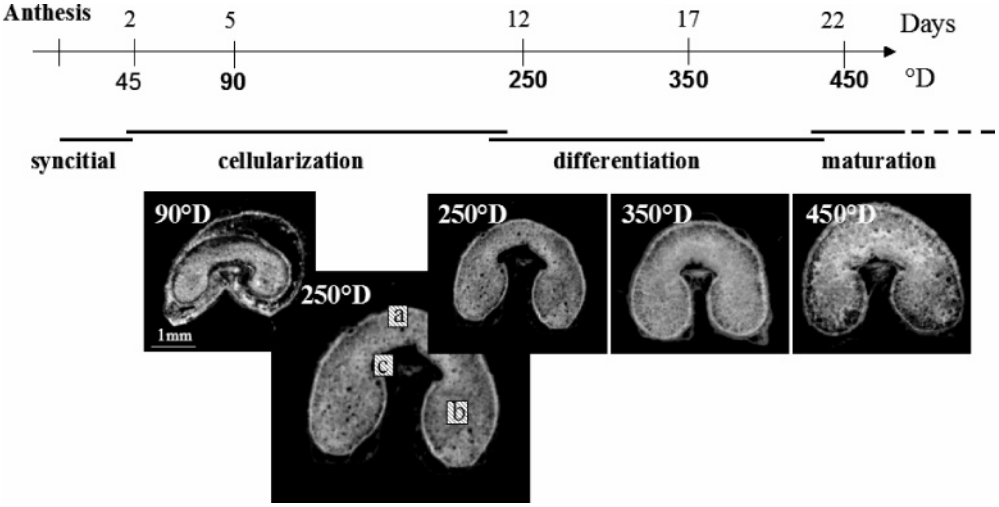

Figure 1. Time course of wheat grain development and transverse sections of wheat grain endosperm (*T. aestivum*) at different development stages. °D, temperature/energy accumulated daily by the grain after anthesis. Mainly four stages of wheat grain development are distinguished according to events that affect embryo and endosperm after anthesis (*26*). Stage 1 is the syncitial period (0–2/3 days after anthesis, DAA), which includes fertilization and the subsequent division of the triploid endosperm nuclei to form a multinucleate cytoplasmic matrix around the periphery of the central cell. Then, gradual formation of cell walls and partition of the original lumen into a characteristic cellular pattern take place during the cellularization period (stage 2, from 2/3 to 12/14 DAA). The next stage (stage 3, from 12/14 to 21/23 DAA) corresponds to cell differentiation, a period for cell expansion in which water content increases and starch and protein reserves accumulate. At this stage, the aleurone layer appears. Stage 4 (from 21/23 to 31 DAA) is the maturation period when the full potential of the grain is realized. Cell expansion and water accumulation stop before the cessation of dry matter accumulation, starch and protein replace cell water, and the kernel begins to desiccate.

observed that not only AX but proteins and lipids play a role in mechanical properties of endosperm cell walls.

The Raman fingerprints of xylan models with (1→4), (1→3), or (1→2) α or β glycosidic links were investigated by Kacurakova et al. (*15*). (1→4) Xylans differing by their degree and nature of substitution were also studied by the authors. In (1→4) xylans the dominant band positions are those of the glycosidic link and ring vibrations at 1125 and 1089 cm^{-1}. In the anomeric region, an absorption band at ≈897 cm^{-1} was assigned to the β (1→4) glycosidic bond of xylans. Except for the remarkable bands of β (1→4) linked backbone, the line width of the Raman spectral bands depends on side substitution by arabinofuranosyl units at the O-3 position. Phenolic acid was revealed by the characteristic doublet band in the 1590−1630 cm^{-1} region. Recently, Barron (*24*) gave a detailed assignment of AX Raman spectra according to their degree of substitution. Linear relationships were observed between the measured degree of substitution and the peak ratios 570/494 and 855/898 cm^{-1}.

In the present paper, Raman microspectroscopy was used to study changes in the degree of substitution with arabinose and changes in the degree of esterification with ferulic acid for AX during wheat grain development. At each stage of wheat grain development, arabinoxylan structural features were more precisely investigated within the different regions of endosperm.

MATERIALS AND METHODS

Biological Materials. Experiments were carried out on a winter wheat (*Triticum aestivum* cv. Recital) provided by INRA Breeding station, Le Rheu (France). The wheat seedlings were vernalized for 2 months in a growth cabinet at 8 °C and light/dark 8/16 h. Then seedlings were transplanted into individual pots in a standard potting mixture (peat RHP15 Klassman, K Klasmann France, Bourgoin Jaillieu, France). After planting, an Osmocote (R) Exact Tablet containing nitrogen (15%), phosphate (9%), potassium hydroxide (9%), and magnesium (3%) (Scotts International B.V., Waardenburg, The Netherland) was added. The plants were watered daily. Following anthesis, mean daily temperatures were recorded, and thermal times [degree days (°D)] were calculated as the summation of mean daily temperature following anthesis minus the base temperature. The base temperature used was 0 °C (*25*). Grains were harvested at four different stages of grain development: 90, 250, 350, and 450 °D (**Figure 1**).

Raman Microspectroscopy. *Sample Preparation.* Wheat grains were picked from the middle third of the ear and stored in 70% ethanol. Sectioning was carried out with a Vibratome (Microm Microtech, FR) in 70% ethanol. Transverse sections 50 μm thick were sonicated in 70% ethanol for 2 min to remove cell contents and more particularly starch (*11*). The sections were thereafter washed in 70% ethanol.

Raman Analysis. Sections were laid onto glass slides and left to dry at room temperature. Cell walls of six endosperm cell types were investigated for each section: from the outer to the inner part of the wheat grain endosperm, aleurone cells, subaleuronic, prismatic cell, and central cells, and; in the crease area, modified aleurone and modified subaleuronic cells (**Figure 2**). Spectra were recorded between 95 and 3927 cm^{-1} using a confocal Raman microspectrometer (Almega, Thermo-Electron) with the following configuration: excitation laser, He−Ne (λ_0 = 633 nm); grating, 500 grooves/mm; pinhole, 25 μm; objective, ×100. The spectral resolution varied between 5 and 9 cm^{-1} according to the spectral region. The acquisition area was about 2 μm × 2 μm. The acquisition time was 10 min per spectrum.

For each stage of grain development, three grains, one section per grain, and five spectra per cell type were recorded. The 350−1800 cm^{-1} spectral region was further smoothed, and baselines were corrected and normalized using OPUS-NT software (version 2.06, Brucker).

Data Treatment. The spectra were split into two regions of interest: the first one considered to be a signature of AX (370−650 cm^{-1}) and the second one a signature of feruloylation of arabinoxylans (800−1800 cm^{-1}).

Principal component analysis (PCA) was then applied to these two selected spectral regions (*27*, *28*). The computation of principal components is based on the diagonalization of the variance−covariance matrix **V** assessed from the spectral data **X**. The diagonalization realizes a decomposition of **V** into eigenvectors **L** and eigenvalues **S**. The eigenvalues describe the amount of total variance taken into account by the principal components. The eigenvectors are used to assess the principal component scores **C**

$$\mathbf{V} = \mathbf{X}'\mathbf{X} \qquad \mathbf{C} = \mathbf{XL}$$

where **X** is the matrix of the spectral data (n samples × m wavenumbers) and **X′** the transpose matrix of **X**.

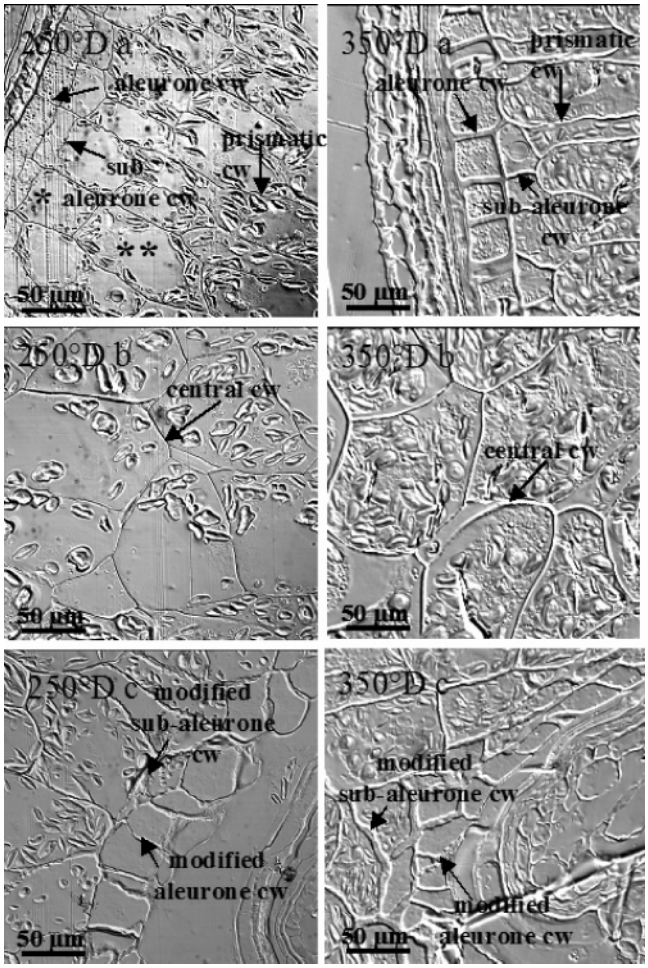

Figure 2. Light microscope images of wheat grain section at 250 and 350 °D showing the different cell types in the endosperm. At 250 °D (**a**), aleurone cells are apparent. They correspond to the small, thin-walled outer cells of the endosperm. The inner daughter cells of aleurone cells, which divide periclinally (**b**), are the source of the so-called subaleurone cells. In the dorsal region, the endosperm cells originally cuboidal (**b***), undergo considerable radial elongation as they become filled with starch and protein reserves (**). The central cells in the center of the cheeks are large and exhibited rounded or polygonal shape. Note the marked size difference between the most recently formed cells (**a***) and the oldest cells in the center (**b**). In the crease region (**c**), the modified aleurone cells are clearly visible and consist of crushed and distorted cells. By 350 °D (**a**), aleurone cells have developed into large isodiametric, thick-walled cells with dense granular content and large nucleus characteristic of mature aleurone layer. The cells in the starchy endosperm are large and thin-walled and become filled with starch granules (**b**, **c**). The subaleurone cells exhibit cuboid shape, and the prismatic cells, about 150 μm long and 50 μm wide, radiate in column (**b**). The central cells tend to retain their shape (**c**). The modified aleurone cell walls have apparently stopped growing, but the walls have increased in thickness. Micrographs **a**, **b**, and **c** correspond to regions a, b, and c on the 250 °D section in **Figure 1**. cw, cell wall.

The principal component scores are used to draw similarity maps that allow a comparison of the spectra with each other. The similarity maps are used to define cell type clusters. Characteristic absorption bands are depicted using the spectral patterns derived from the eigenvectors and were used to extract structural information on the arabinosyl substitution and the degree of feruloylation of arabinoxylans.

Variance analyses (ANOVA, Statgraphics Plus 3.0, SigmaPlus) were carried out on Raman data to investigate the effect of cell type, the effect of grain development stage, and the interaction between cell type and grain development stage. Multiple-comparison analysis was applied to the data to determine which means for each level of the factors (cell types and grain development stage) are significantly different.

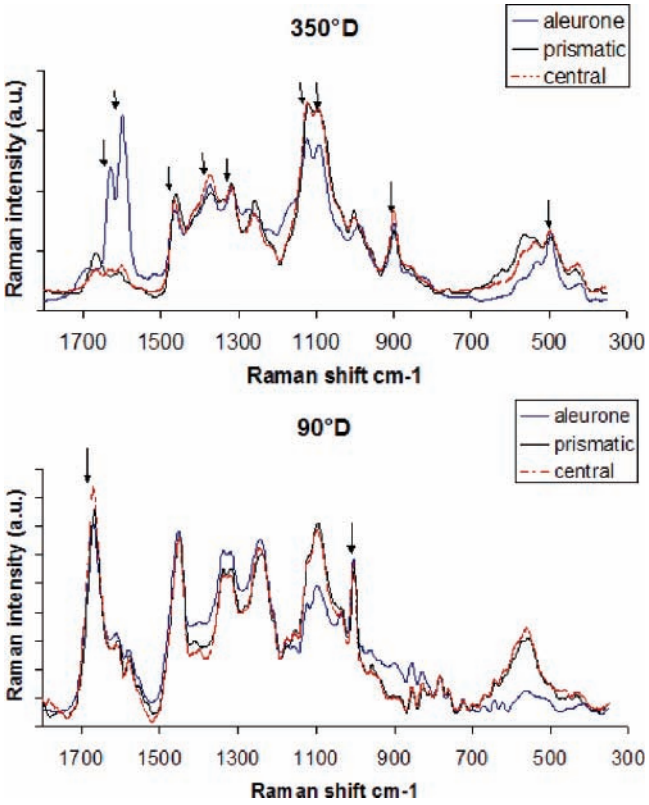

Figure 3. Micro-Raman spectra of endosperm cell walls: (**a**) at 350 °D (grain filling); (**b**) at 90 °D (end of cellularization).

RESULTS AND DISCUSSION

General Assignment. Typical Raman spectra of wheat grain endosperm cell wall recorded for different regions of wheat grain harvested at 350 °D are shown in **Figure 3a**. Raman bands characteristic of AX were observed at 493, 896, 1091, 1123, 1316, 1370, and 1462 cm^{-1} (*22*, *23*). Whereas the 1400−1300 cm^{-1} spectral region could be assigned to CH and COH bending, COC, CO, and CC stretching was observed in the 1000−1200 cm^{-1} range. The presence of β (1→4) glycosidic linkage was identified by the Raman band at 896 cm^{-1}. The relative band intensities in the 400−600 cm^{-1} were previously used to assess the degree of substitution of the xylan chain by arabinose units (*24*). Besides the arabinoxylan bands, the Raman spectra of aleurone layers revealed bands characteristic of phenolic compounds at 1628 and 1598 cm^{-1}. These bands were assigned to ferulic acid as it is predominant in wheat endosperm (*9*, *10*). A frequency shift of the doublet between pure ferulic acid (1603 and 1630 cm^{-1}) and ferulic acid in aleurone layers could be noted. The shift was assigned to an esterified form of ferulic acid in cell walls (*21*).

Spectra recorded at 90 °D (**Figure 3b**) differed from those obtained at 250, 350, and 450 °D. Strong diffusion bands were observed at 1667 and 1001 cm^{-1} that might be assigned to protein (*21*). Due to the low diffusion intensity observed, detailed assignment of these spectra could not be carried out. However, no spatial heterogeneity of Raman features could be detected. Our previous results showed that arabinoxylans were almost absent from cell walls at this early stage (*12*). As the main focus of the present paper was on AX, the 90 °D stage was discarded from further analysis. Raman spectra of wheat

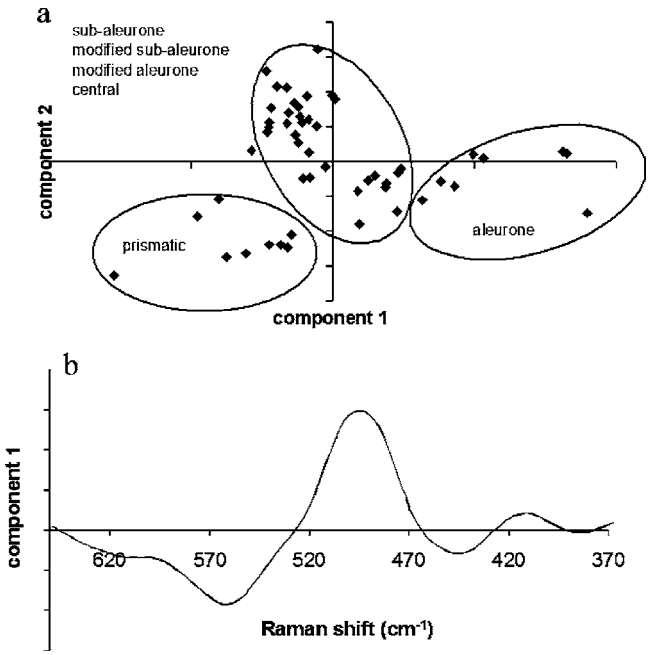

Figure 4. PCA applied to endosperm cell walls at 350 °D: (**a**) similarity map of micro-Raman spectra recorded between 370 and 650 cm^{-1}; (**b**) spectral pattern derived from principal component 1.

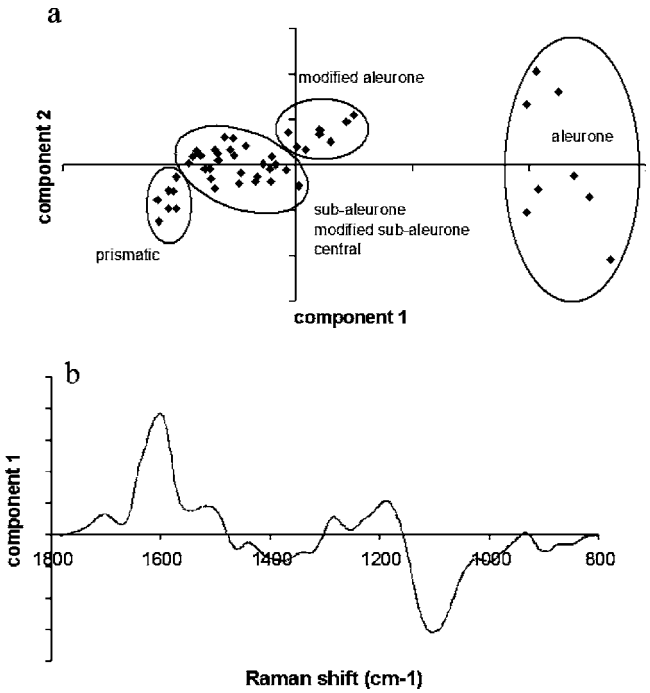

Figure 5. PCA applied to endosperm cell walls at 350 °D: (**a**) similarity map of micro-Raman spectra recorded between 800 and 1800 cm^{-1}; (**b**) spectral pattern derived from component 1.

endosperm cell walls recorded at 350 °D were compared by applying PCA.

For the 370−650 cm^{-1} spectral region, the first two principal components explained >85% of the total variance and were retained to draw a similarity map (**Figure 4a**). Prismatic cell walls were identified by negative scores, whereas aleurone cell walls were characterized by positive scores along principal component 1. The loading plot associated with principal component 1 made it possible to explore the spectral features that discriminated the samples (**Figure 4b**). The spectral pattern or loading plot revealed a negative peak around 570 and a positive peak at ≈490 cm^{-1}. Barron et al. (*24*), using a set of AX and oligosaccharides exhibiting variation in the degree of substitution, found that the specific diffusion bands at around 570 and 490 cm^{-1} were indicative of the arabinosyl substitution of AX. The results derived from PCA indicated that the degree of substitution of AX was lower in aleurone cell walls than in starchy endosperm cell walls. They clearly highlighted a higher degree of substitution of AX in prismatic cell walls.

For the 800−1800 cm^{-1} spectral region, the first two principal components took >90% of total inertia into account. The aleurone and prismatic cell walls were again clearly identified along principal component 1 (**Figure 5a**). The principal component loading 1 showed a positive peak at 1600 cm^{-1} related to ferulic compounds (**Figure 5b**). A negative peak at 1094 cm^{-1} could be assigned to AX. Results derived from PCA revealed that aleurone cell walls presented the highest amount of esterified ferulic compounds. Interestingly, modified aleurone cell walls differed from the aleurone ones and were poorer in esterified ferulic acid. The lowest feruloylation of AX was observed for prismatic cell walls. Feruloylation of AX in the central, subaleurone, and modified subaleuronic cell walls was close to that observed in prismatic cell walls.

PCA indicated that the assessment of intensity ratios could be sufficient to estimate arabinoxylan substitution (570 cm^{-1}/490 cm^{-1}) and ferulic acid esterification (1600 cm^{-1}/1094 cm^{-1}).

Temporal and Spatial Deposition of Cell Wall Polymers. The 570 cm^{-1}/490 cm^{-1} intensity ratios were calculated at 250, 350, and 450 °D for each cell type (**Figure 6**). Whatever the cell type, higher arabinoxylan substitution was obtained at 250 °D. In addition, whatever the stage of wheat grain development, AX were most substituted in the walls of prismatic cells and least substituted in the walls of aleurone cells. Variance analysis was applied to the intensity ratios to highlight differences between cell types and stages of development. The effect of stage development as well as the effect of cell type and the interaction between cell type and stage development was found to be significant at a level of 5%. The least significant difference method (LSD) used for mean comparison showed that the 250 °D stage significantly differed from the 350 and 450 °D stages. The LSD procedure specified that cell types could be divided into four clusters according to arabinoxylan substitution (**Table 1**). Aleurone, prismatic, modified aleurone, and modified subaleurone cells clearly belonged to distinct groups. On the other hand, central and subaleurone cells merged with modified aleurone and subaleurone cells and therefore belonged to mixed clusters (bc). The interaction effect between cell type and development stage was mainly due to prismatic cells: the arabinoxylan substitution decreased drastically between 250 and 350 °D (see **Figure 6**).

Our results clearly showed that AX in endosperm were more substituted at the 250 °D development stage in comparison with the later stages. This would suggest that either AX are delivered in the cell wall in a highly substituted form and then remodeled through the action of arabinoxylan arabinofuranohydrolases or little substituted AX are incorporated into the wall late in cell wall development, making the average value for degree of AX substitution decreased. Remodeling through action of arabinoxylan arabinofuranohydrolases has been previously reported in barley coleoptile during growth and development (*29*).

Spatial changes in the degree of substitution were observed within the endosperm. AX originated from the aleurone layer are characterized by a low degree of substitution compared to cells of the starchy endosperm, as expected from the literature (*7*, *10*). At 250 °D, from a morphological point of view, the

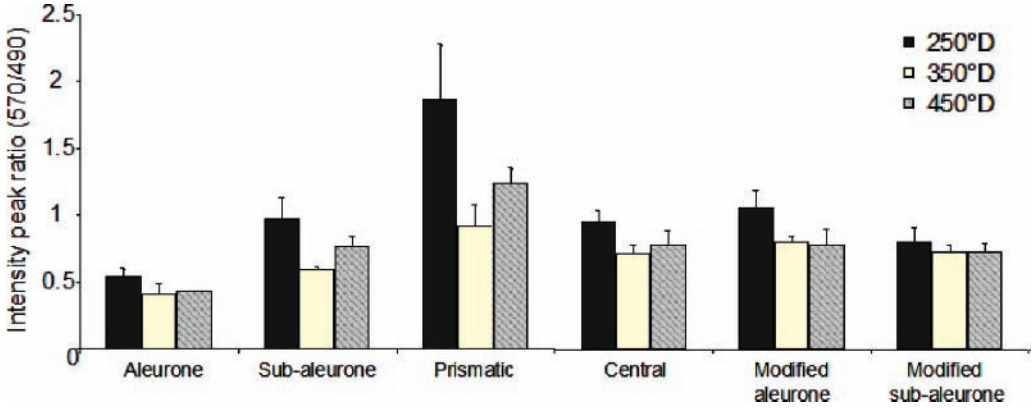

Figure 6. Peak intensity ratio $I_{570cm^{-1}}/I_{490\ cm^{-1}}$ as an indicator of the arabinoxylan degree of substitution. Values represent the means of three grains (bar, mean confidence interval).

Table 1. Multiple-Range Tests for the Peak Intensity Ratio $I_{570cm^{-1}}/I_{490cm^{-1}}$ by Cell Type (LSD Method at $P = 0.05$)

cell type	homogeneous groups[a]
aleurone	a
modified subaleurone	b
subaleurone	bc
central	bc
modified aleurone	c
prismatic	d

[a] Groups with the same letter are not significantly different.

subaleurone cell looked much more like aleurone cells (**Figure 2**). However, the cell walls and in particular AX exhibited some differences, suggesting that the cell fate was already programmed. The morphology of modified aleurone cells was quite different from that of their counterparts in the dorsal region, with cuboidal shape and thicker cell walls. These cells did not undergo divisions as did those in the dorsal region. They are already differentiated and probably functioned as groove aleurone cells (*30*). Interestingly, AX in modified aleurone cells appeared to be more similar in terms of arabinose subtitution to AX in central and modified subaleurone cells than to AX in aleurone cell walls. Within the starchy endosperm, AX appeared to be more substituted in the case of prismatic cell walls. Philippe et al. (*12*), using immunocytochemistry, showed that cell walls in the peripheral starchy endosperm reacted less with arabinoxylan antibodies against little substituted AX than cell walls in the central starchy endosperm. Barron et al. (*11*), using FTIR microspectroscopy, reported differences between peripheral and central starchy endosperm cell walls, but without relating the differences to arabinoxylan substitution. At the early stage, cell division occurs mainly in the layer just within the outermost layer, which subsequently differentiated into the aleurone layer. Therefore, the prismatic cells are generated after the central ones. The higher degree of AX substitution of prismatic cells at the early stage of development could be explained by the fact that they are younger. The distinction between prismatic and central cells remained visible at later stages of development. The position of cells within the endosperm in some way seemed to play a role in the cell fate. To date, the spatial and temporal changes of arabinxylan substitution are not understood.

Ferulic acid content in cell wall endosperm was estimated by assessing the 1600 cm^{-1}/1094 cm^{-1} intensity ratio (**Figure 7**). The amount of esterified ferulic acid increased between 250 and 350 °D, especially in the case of aleurone cell walls. At all development stages of wheat grain, the ferulic acid content was higher in the aleurone layer than in the other endosperm regions. Variance analysis was applied to the intensity ratios to highlight differences according to the cell types and stages of development. The effect of stage development as well as the effect of cell type and the interaction between cell type and stage development were found to be significant at a level of 5%. The LSD method used for mean comparison confirmed that the 250 °D stage significantly differed from the 350 and 450 °D stages. At 250 °D, the feruloylation of AX was low, even in the case of the aleurone layer. Past 350 °D, no further increase in the feruloylation of AX was observed. The LSD procedure specified that cell types could be divided into three clusters according to

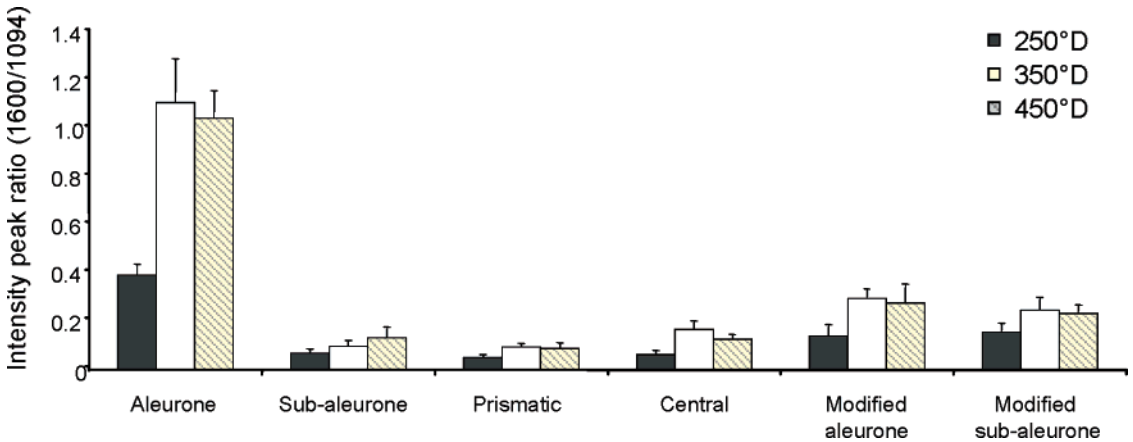

Figure 7. Peak intensity ratio $I_{1600cm^{-1}}/I_{1094cm^{-1}}$ as an indicator of the feruloylation of AX. Values represent the means of three grains (bar, mean confidence interval).

Table 2. Multiple-Range Tests for the Peak Intensity Ratio $I_{1600cm^{-1}}/I_{1094cm^{-1}}$ by Cell Type (LSD Method at $P = 0.05$)

cell type	homogeneous groups[a]
prismatic	a
subaleurone	a
central	a
modified subaleurone	b
modified aleurone	b
aleurone	c

[a] Groups with the same letter are not significantly different.

the amount of esterified ferulic acid (**Table 2**). Subaleurone, prismatic, and central cells clearly belonged to the same group and were characterized by a low amount of esterified ferulic acid. Aleurone cells with their high content in esterified ferulic constituted one group. The last group included modified subaleurone and modified aleurone cells. In this group, AX presented intermediate amounts of esterified ferulic acid. The interaction effect of cell type and development stage was significant: the effect of development was particularly obvious for the aleurone cells (see **Figure 7**). Aleurone cell walls are heavily esterified compared to those of the starchy endosperm. This has been well established in mature grain (*6*, *8*, *9*, *10*, *22*, *31*, *32*). In agreement with Fulcher et al. (*33*), we demonstrated that esterification occurred as soon as 250 °D and was amplified between 250 and 350 °D. The AX in the aleurone walls in the crease region were different. The occurrence of phenolic compounds in the modified aleurone cell walls has been followed since the early development stage and subsequent differentiation of endosperm using fluorescence microscopy (*34*). Whereas at 10 days after anthesis (≈250 °D) cells fluoresced quite intensely throughout the walls, at maturity, the fluorescence was restricted to the inner wall layer of cell. The low esterification of AX in modified aleurone cell observed in the present paper could be, therefore, ascribed to a restricted location of phenolic compounds.

The increase in arabinoxylan esterification and in particular for aleurone cells between 250 and 350 °D corresponded to a dramatic change in the cell morphology. Aleurone cells develop into large isodiametric and thick-walled cells. Dimerization of ferulic acid could cross-link AX and therefore strengthen cell walls. The next step will be to look more precisely to the presence of dimers on the course of aleurone differentiation and development.

Confocal Raman microspectrocopy allows spatially resolved study and is sensitive to structural arabinoxylan features. In the present study, it was used to investigate changes in arabinoxylan fine structure during grain development and across the endosperm itself. The grains were from plants cultivated under controlled and continuous environmental conditions. It could be of great interest to study the impact of environmental conditions and of endosperm hardness on arabinoxylan structural features.

ABBREVIATIONS USED

AX, arabinoxylans; A/X, molar ratio of arabinose to xylose; DAA, days after anthesis; WE, water extractable.

ACKNOWLEDGMENT

We thank Maxime Trottet and Françoise Dedryver (UMR Amélioration des Plantes et Biotechnologies Végétales, INRA Rennes, France) for the culture and supply of wheat grain.

LITERATURE CITED

(1) Fincher, G. B.; Stone, B. A. Cell walls and their components in cereal grain technology. In *Advances in Cereal Science and Technology*; Pomeranz, Y., Ed.; American Association of Cereal Chemists: St. Paul, MN, 1986; pp 207−295.

(2) Courtin, C. M.; Delcour, J. A. Arabinoxylans and endoxylanases in wheat flour bread-making. *J. Cereal Sci.* **2002**, *35*, 225−243.

(3) Andersson, R.; Westerlund, E.; Aman, P. Natural variations in the contents of structural elements of water-extractable non starch polysaccharides in white flour. *J. Cereal Sci.* **1994**, *19*, 77−82.

(4) Cleemput, G.; Vanoort, M.; Hessing, M.; Bergmans, M. E. F.; Gruppen, H.; Grobet, P. J.; Delcour, J. A. Variation in the degree of D-xylose substitution in arabinoxylans extracted from a European wheat-flour. *J. Cereal Sci*. **1995**, *22*, 73−84.

(5) Delcour, J. A.; Van Win, H.; Grobet, P. J. Distribution and structural variation of arabinoxylans in common wheat mill streams. *J. Agric. Food Chem.* **1999**, *47*, 271−275.

(6) Dervilly, G.; Saulnier, L.; Roger, P.; Thibault, J.-F. Isolation of homogeneous fractions from wheat water-soluble arabinoxylans. Influence of the structure on their macromolecular characteristics. *J. Agric. Food Chem.* **2000**, *48*, 270−278.

(7) Ordaz-Ortiz, J. J.; Saulnier, L. Structural variability of arabinoxylans from wheat flours. Comparison of water-extractable and xylanase-extractable arabinoxylans. *J. Cereal Sci.* **2005**, *42*, 119−125.

(8) Bacic, A.; Stone, B. A. Isolation and ultrastructure of cell walls from wheat and barley. *Aust. J. Plant Physiol.* **1981**, *8*, 453−474.

(9) Rhodes, D. I.; Sadek, M.; Stone, B. A. Hydroxycinnamic acids in walls of wheat aleurone cells. *J. Cereal Sci.* **2002**, *36*, 67−81.

(10) Antoine, C.; Peyron, S.; Mabille, S.; Lapierre, C.; Bouchet, C.; Abecassis, J.; Rouau, X. Individual contribution of grain outer layers and their cell wall structure to the mechanical properties of wheat bran. *J. Agric. Food Chem.* **2003**, *51*, 2026−2033.

(11) Barron, C.; Parker, M. L.; Mills, E. N. C.; Rouau, X.; Wilson, R. H. FTIR imaging of wheat endosperm cell walls *in situ* reveals compositional and architectural heterogeneity related to grain hardness. *Planta* **2005**, *220*, 667−677.

(12) Philippe, S.; Saulnier, L.; Guillon, F. Arabinoxylans and β-glucans deposition in cell wall during wheat endosperm development. *Planta* **2006**, in press.

(13) Lin-Vien, D.; Colthup, N. B.; Fateley, W. G.; Grasselli J. G. *The Handbook of Infrared and Raman Characteristic Frequencies of Organic Molecules*; Academic Press: San Diego, CA, 1991.

(14) Jarvis, M. C.; McCann, M. C. Macromolecular biophysics of the plant cell wall: concepts and methdology. *Plant Physiol. Biochem.* **2000**, *38*, 1−13.

(15) Kacurakova, M.; Wellner, N.; Ebringerova, A.; Hromadkova, Z.; Wilson, R. H.; Belton, P. S. Characterisation of xylan-type polysaccharides and associated cell wall components by FT-IR and FT-Raman spectroscopies. *Food Hydrocolloids* **1999**, *13*, 35−41.

(16) Ma, C. Y.; Phillips, D. L. FT-Raman spectroscopy and its applications in cereal science. *Cereal Chem.* **2002**, *79*, 171−177.

(17) Agarwal, U. P.; Atalla, R. H. *In situ* Raman microprobes studies of plant cell walls: macromolecular organization and compositional variability in the secondary wall of *Picea mariana* (Mill.) B.S.P. *Planta* **1986**, *169*, 325−332.

(18) Atalla, R. H.; Agarwal, U. P. Recording Raman spectra from plant cell walls. *J. Raman Spectrosc.* **1986**, *17*, 229−231.

(19) Atalla, R. H. Raman spectroscopy and the Raman microprobe: valuable tools for characterizing wood and pulp fibers. *J. Wood Chem. Technol.* **1987**, *7*, 115−131.

(20) Séné, C. F. B.; McCann, M. C.; Wilson, R. H.; Grinter, R. Fourier-transform Raman and Fourier transform infrared spectroscopy—an investigation of 5 higher plant cell-walls and their components. *Plant Physiol.* **1994**, *106*, 1623−1631.
(21) Piot, O.; Autran, J.-C.; Manfait, M. Spatial distribution of protein and phenolic constituents in wheat grain as probed by confocal Raman spectroscopy. *J. Cereal Sci.* **2000**, *32*, 57−71.
(22) Piot, O.; Autran, J.-C.; Manfait, M. Investigation by confocal Raman microspectroscopy of the molecular factors responsible for grain cohesion in the *Triticum aestivum* bread wheat. Role of the cell walls in the starchy endosperm. *J. Cereal Sci.* **2001**, *34*, 191−205.
(23) Thygesen, L. G.; Løkke, M. M.; Micklander, E.; Engelsen, S. Vibrational microspectroscopy of food. Raman vs FT-IR. *Trends Food Sci. Technol.* **2003**, *14*, 50−57.
(24) Barron, C.; Robert, P.; Guillon, F.; Saulnier, L.; Rouau, X. Structural heterogeneity of wheat arabinoxylans revealed by Raman spectroscopy. *Carbohydr. Res.* **2006**, online.
(25) McMaster, G. S.; Wilhem, W. W. Growing degree-days: one equation, two interpretations. *Agric. For. Meteorol.* **1997**, *87*, 291−300.
(26) Simmonds, D. H.; O'Brien, T. P. Morphological and biochemical development of the wheat endosperm. In *Advances in Cereal Science and Technology*; Pomeranz, Y., Ed.; American Association of Cereal Chemists: St. Paul, MN, 1981; Vol. IV, pp 5−70.
(27) Cowe, I. A.; McNicol, J. W. The use of principal component in the analysis of near infrared spectra. *Appl. Spectrosc.* **1985**, *39*, 257−265.
(28) Robert, P.; Devaux, M.-F.; Bertrand, D. Beyond prediction: extracting relevant information from near infrared spectra. *J. Near Infrared Spectrosc.* **1996**, *4*, 75−84.
(29) Gibeaut, D. M.; Pauly, M.; Bacic, A.; Fincher, G. F. Changes in cell wall polysaccharides in developing barley (*Hordeum vulgare*) coleoptiles. *Planta* **2005**, *221*, 729−738.
(30) Olsen, O.-A.; Linnestsa, C.; Nichols, S. E. Developmental biology of the cereal endosperm. *Trends Plant Sci.* **1999**, *4*, 253−257.
(31) Akin, D. E. Microspectrophotometric characterization of aromatic constituents in cell walls of hard and soft wheats. *J. Sci. Food Agric.* **1995**, *68*, 207−214.
(32) Saadi, A.; Lempereur, I.; Sharonov, S.; Autran, J. C.; Manfait, M. Spatial distribution of phenolic materials in durum wheat grain as probed by confocal fluorescence spectral imaging. *J. Cereal Sci.* **1998**, *28*, 107−114.
(33) Fulcher, R. G.; O'Brien, T. P.; Lee, J. W. Studies on the aleurone layer. I: Conventional and fluorescence microscopy of the cell wall with emphasis on phenol−carbohydrate complexes in wheat. *Aust. J. Biol. Sci.* **1972**, *25*, 23−24.
(34) Morrison, I. N.; O'Brien, T. P.; Kuo, J. Initial cellularization and differentiation of the aleurone cells in the ventral region of developing wheat grain. *Planta* **1978**, *140*, 19−30.

Received for review February 16, 2006. Revised manuscript received May 10, 2006. Accepted May 11, 2006.

JF060466M